Bioconjugate Chemistry

Article

pubs.acs.org/bc

Conjugation of Cell-Penetrating Peptides to Parathyroid Hormone Affects Its Structure, Potency, and Transepithelial Permeation

Mie Kristensen,[†] Anne Marit de Groot,[§] Jens Berthelsen,[‡] Henrik Franzyk,[∥] Alice Sijts,[§] and Hanne Mørck Nielsen*,[†]

[†]Section for Biologics, Department of Pharmacy, Faculty of Health and Medical Sciences, University of Copenhagen, Universitetsparken 2, DK-2100 Copenhagen, Denmark

[‡]Department of International Health, Immunology and Microbiology, Faculty of Health and Medical Sciences, University of Copenhagen, Blegdamsvej 3, DK-2200 Copenhagen, Denmark

[§]Division of Immunology, Department of Infectious Diseases and Immunology, Faculty of Veterinary Medicine, Utrecht University. Yalelaan 1, 3584 CL Utrecht, The Netherlands

[∥]Department of Drug Design and Pharmacology, Faculty of Health and Medical Sciences, University of Copenhagen, Universitetsparken 2, DK-2100 Copenhagen, Denmark

Supporting Information

ABSTRACT: Delivery of therapeutic peptides and proteins by the use of cell-penetrating peptides (CPPs) as carriers has been suggested as a feasible strategy. The aim of the present study was to investigate the effect of conjugating a series of well-known CPPs to the biologically active part of parathyroid hormone, i.e., PTH(1−34), and to evaluate the effect with regard to secondary structure, potency in Saos-2 cells, immunogenicity, safety, as well as the transepithelial permeation across monolayers by using the Caco-2 cell culture model. Further, co-administration of CPP and PTH(1−34) as an alternative to covalent conjugation was compared with regard to the transepithelial permeation. CPP-conjugated PTH(1−34) fusion peptides were successfully expressed in *Escherichia coli* and purified from inclusion bodies. No clear correlation between the degree of secondary structure of the CPP-conjugated PTH(1−34) fusion peptides and their potency was found, albeit a general decrease in permeation was observed for both N- and C-terminally CPP-conjugated PTH(1−34) as compared to native PTH(1−34). However, attachment of CPP to the N-terminus significantly increased permeation across Caco-2 cell monolayers as compared to the corresponding C-terminally CPP-conjugated PTH(1−34). In addition, the nonaarginine sequence proved to be the only CPP capable of increasing permeation when conjugated to PTH(1−34) as compared to co-administration of CPP and PTH(1−34). This enhancement effect was, however, associated with an unacceptably low level of cell viability. In conclusion, covalent conjugation of CPPs to PTH(1−34) influenced the secondary structure, potency, and transepithelial permeation efficiency of the resulting conjugate, and hence this approach appears not to be favorable as compared to co-administration when optimizing CPP-mediated permeation of PTH(1−34) across an intestinal epithelium.

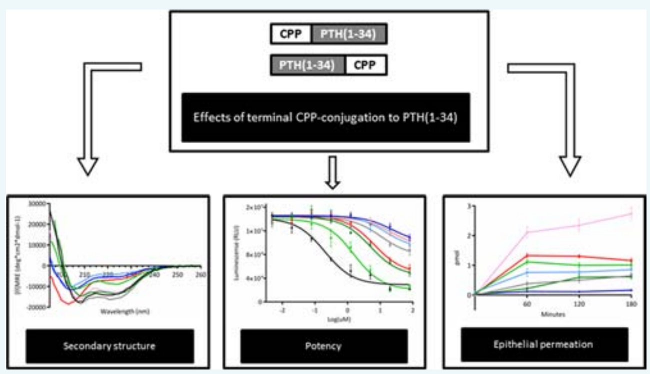

■ INTRODUCTION

Peptides and proteins play important roles as substrates, receptor ligands, downstream signaling molecules, and regulators in a vast number of biological processes, and today they constitute an increasing fraction of drugs used to treat a variety of diseases. Examples comprise use in hormone replacement therapies for, e.g., growth hormone deficiency,[1] and relief of menopausal symptoms in women.[2] Parathyroid hormone (PTH) is an 84-residue protein regulating bone and renal metabolism through its action as a regulator of the extracellular Ca^{2+} level.[3] The N-terminal part comprising 34 residues, i.e., PTH(1−34), is responsible for the pharmacological activity,[4] and today this peptide is used clinically in the treatment of osteoporosis.[5] This disease is characterized by a decreased bone density and associated with a high risk of fractures leading to impaired mobility, pain, and consequently reduced quality of life for the patients. As with the majority of peptide and protein drugs, PTH(1−34) is currently administered via injections, although oral administration is preferred for optimal patient compliance. However, successful oral delivery of peptide and protein drugs involves overcoming a range of challenges due to their susceptibility toward enzymatic

Received: December 8, 2014
Revised: January 19, 2015
Published: January 22, 2015

Table 1. Sequence and Molecular Weight of the Expressed and Purified PTH(1−34) and CPP-Conjugated PTH(1−34) Fusion Peptides[a]

name	sequence	Calc. Mw (Da)	Mw (Da)
PTH(1−34)	S*SVSEIQLMHNLGKHLNSMERVEWLRKKLQDVHNF	4204.84	4204.19
PTH(1−34)-penetratin	S*SVSEIQLMHNLGKHLNSMERVEWLRKKLQDVHNFRQIKIWFQNRRMKWKK	6433.58	6432.35
PTH(1−34)-Tat	S*SVSEIQLMHNLGKHLNSMERVEWLRKKLQDVHNFYGRKKRRQRRR	5746.67	5746.10
Tat-PTH(1−34)	SS*YGRKKRRQRRRSVSEIQLMHNLGKHLNSMERVEWLRKKLQDVHNF	5833.75	5833.13
PTH(1−34)-VP22	S*SVSEIQLMHNLGKHLNSMERVEWLRKKLQDVHNFDAATATRGRSAASRPTERPRAPARSASRPRRPVG	7773.81	7773.10
VP22-PTH(1−34)	SS*DAATATRGRSAASRPTERPRAPARSASRPRRPVGSVSEIQLMHNLGKHLNSMERVEWLRKKLQDVHNF	7860.89	7864.13
PTH(1−34)-R9	S*SVSEIQLMHNLGKHLNSMERVEWLRKKLQDVHNFRRRRRRRRR	5610.53	5607.08
R9-PTH(1−34)	SS*RRRRRRRRRSVSEIQLMHNLGKHLNSMERVEWLRKKLQDVHNF	5697.60	5694.12

[a]The CPP sequences are underlined. *N-terminal serine (Ser) residues left on the amino acid sequence encoding PTH(1−34) or on the linked CPP after the His tag was cleaved off by a TEV-specific protease. Nucleotide encoding sequences with an inherent N-terminal Ser residue were ordered without the Ser residue. Calculated molecular weights are obtained from Expasy.org.

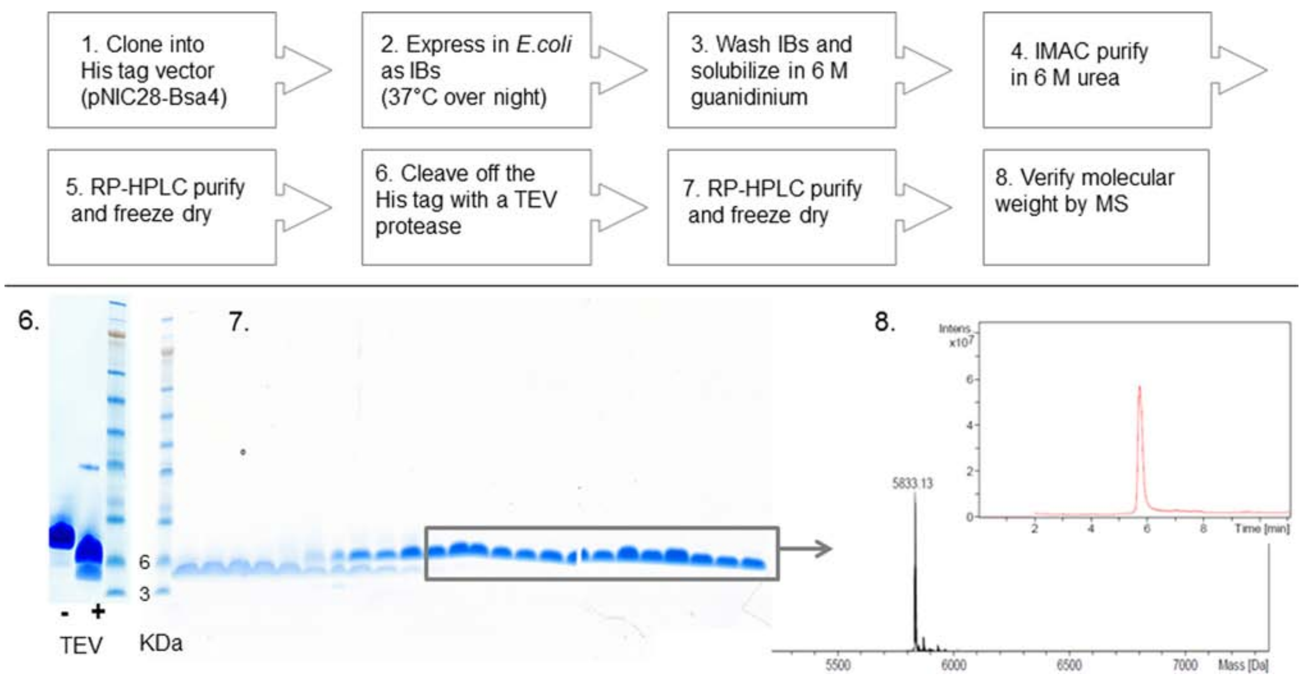

Figure 1. Representative expression and purification of Tat-PTH(1−34) including flowchart (steps 1−8, top) and experimental results (6−8, bottom) of TEV cleavage (6), RP-HPLC purification (7) and MS (8). IB: Inclusion body.

degradation, their large molecular size, and thus poor membrane permeation. To circumvent these obstacles, carriers are obviously needed; thus, utilization of cell-penetrating peptides (CPPs) as delivery vehicles appears to be a possible solution, as they have shown promising potential in improving transepithelial delivery of therapeutic peptides and protein drugs[6] either when co-administered with the therapeutic[7−9] or via direct conjugation to the drug.[10,11]

In the latter case, a CPP is covalently linked to the therapeutic peptide or protein either by chemical synthesis, e.g., as reported for the conjugation of Tat to insulin via the Lys residue B29 in insulin,[10] or by bacterial expression, e.g., as reported for N-terminally CPP-fused α-synuclein.[6,11−13] The use of an expression host, such as *Escherichia coli* (*E. coli*), enables production of a recombinant fusion peptide, in which gene fragments encoding separate functional parts are translated into a fusion peptide. This approach ensures an inherent proximity of the CPP to the therapeutic peptide or protein, and leads to well-characterized molecules, thus limiting the potential formation of poorly characterized complexes as a result of physical mixing of excess CPP with the therapeutic peptide. However, knowledge regarding the effect of the CPP on the pharmacological activity of the therapeutic peptide or protein as well as the influence of conjugation on the cell-penetrating ability of the CPP has been limited so far.

In order to investigate the effect of direct conjugation of CPPs to a therapeutic peptide, the peptide PTH(1−34) was expressed as fusion peptides with a series of well-known CPPs; namely, penetratin (a 16-mer derived from the Antennapedia homeodomain),[14] $Tat_{(47-57)}$ (a 11-mer derived from the HIV-1 transactivating protein),[15] VP22 (a 34-mer derived from the HSV-1 structural protein),[16] and the synthetic nonaarginine (R9).[17] Both N- and C-terminally CPP-conjugated PTH(1−34) fusion peptides were expressed, purified, and characterized with respect to secondary structure, immunogenicity, potency, safety, and ability to permeate across Caco-2 cell monolayers. Finally, co-administration of PTH(1−34) and each of the CPPs in a 1:1 molar ratio was explored in order to directly evaluate to which extent a similar amount of free CPP might facilitate permeation in comparison to the covalently CPP-mediated

DOI: 10.1021/bc5005763
Bioconjugate Chem. 2015, 26, 477−488

approach for enhancing transepithelial transport of PTH(1−34).

RESULTS

Purification of PTH(1−34) and CPP-PTH(1−34) Fusion Peptides from Inclusion Bodies. In order to obtain the designed recombinant CPP-conjugated PTH(1−34) fusion peptides (Table 1), entry clones encoding sequences of interest were cloned into the pNIC-Bsa4 vector (Supporting Information Figure S1) and expressed as the corresponding histidine (His) tagged peptides in *E. coli*. The His tagging facilitated an initial purification step using immobilized metal ion chromatography (IMAC), and expression together with an adjacent tobacco etch virus (TEV) sequence allowed subsequent removal of the tag by using a TEV-specific protease.

As only three of the target sequences were expressed as soluble peptides (Supporting Information Figure S2), a protocol for the purification from insoluble inclusion bodies (IBs) was developed (Figure 1, top). This newly designed protocol enabled efficient expression of PTH(1−34) and the CPP-conjugated PTH(1−34) fusion peptides into IBs, from which purification was carried out by using IMAC followed by two RP-HPLC purification steps. Between the two latter purification steps, the His tag was cleaved off by a TEV-specific protease, and finally the expected molecular weight was verified by mass spectrometry (MS) as exemplified in Figure 1 (bottom) for the Tat-PTH(1−34) fusion peptide.

In total, PTH(1−34) and seven different CPP-conjugated PTH(1−34) fusion peptides were successfully produced, and isolated with an initial high degree of purity as visualized by a Coomassie-stained sodium dodecyl sulfate polyacrylamide gel electrophoresis (SDS-PAGE) (Figure 2). The penetratin sequence could only be successfully expressed when C-terminally conjugated to PTH(1−34), whereas Tat, VP22, and R9 sequences were all successfully expressed both as N- and C-terminal PTH(1−34) conjugates (Table 1).

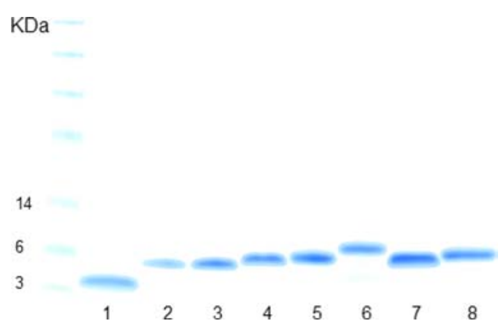

Figure 2. Coomassie-stained SDS-PAGE gel loaded with purified PTH(1−34) and CPP-PTH(1−34) fusion peptides including a prestained molecular weight marker: 1, PTH(1−34); 2, PTH(1−34)-penetratin; 3, PTH(1−34)-Tat; 4, Tat-PTH(1−34); 5, PTH(1−34)-VP22; 6, VP22-PTH(1−34); 7, PTH(1−34)-R9; 8, R9-PTH(1−34).

Folding Propensity of PTH(1−34) and Its Fusion Peptides Is Affected by Lipid Bilayers. An α-helical structure is believed to be of importance for retained potency of PTH(1−34)[18] and may also positively affect plasma membrane interactions of the CPPs.[19,21] Hence, the secondary structure of PTH(1−34) (Figure 3) and of the CPP-conjugated PTH(1−34) fusion peptides (Figure 4) was analyzed by circular dichroism (CD) spectroscopy in the absence or presence of POPC:POPG liposomes as a simplified model for the eukaryote plasma membrane.

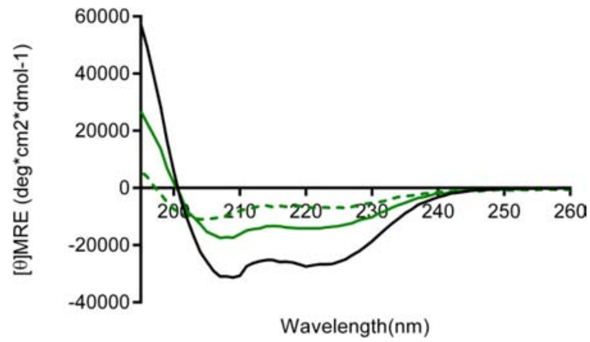

Figure 3. Circular dichroism spectra of PTH(1−34) recorded at a concentration of 10 μM in aqueous buffer (green dashed line), in the presence of 1 mM POPC:POPG (molar ratio 80:20) liposomes corresponding to a 1:100 peptide to lipid ratio (green solid line), or in 20% (v/v) aqueous TFE (black line).

In aqueous buffer, PTH(1−34) did not adopt a clearly defined secondary structure, whereas in the presence of POPC:POPG liposomes, its helicity was increased. Similarly, a high helicity was observed in the presence of 20% (v/v) 2,2,2-trifluoroethanol (TFE), which is widely used as an α-helix-inducing agent (Figure 3).

As seen for PTH(1−34), the structures of the CPP-conjugated PTH(1−34) fusion peptides were not clearly defined in aqueous buffer (Supporting Information Figure S3a), whereas in the presence of 20% (v/v) aqueous TFE, all of the fusion peptides adopted an α-helical structure albeit not to the same extend as observed for PTH(1−34) (Supporting Information Figure S3b). In the presence of POPC:POPG liposomes, conjugation of penetratin to the C-terminus of PTH(1−34) (Figure 4a) did not affect the secondary structure as compared to that of native PTH(1−34) (Figure 3), and neither did C-terminal conjugation of Tat (Figure 4b) or N-terminal conjugation of R9 to PTH(1−34) (Figure 4d). On the other hand, a significant difference was observed when comparing the spectra of N- versus C-terminally conjugation of R9 to PTH(1−34) (Figure 4d), whereas only a minor effect of N- versus C-terminal conjugation was observed for the Tat peptide (Figure 4b), and no effect was seen as a result of N- versus C-terminal VP22-conjugation to PTH(1−34) (Figure 4c). CD spectra of the individual CPPs (Supporting Information Figure S4) revealed that only penetratin adopted an α-helical structure in the presence of POPC:POPG liposomes (Supporting Information Figure S4a) in accordance with previous reports.[20,21]

Decreased Potency of CPP-Conjugated PTH(1−34) Fusion Peptides. The potencies of the CPP-conjugated PTH(1−34) fusion peptides were evaluated in a cell-based PTH assay, using the PTH receptor-expressing Saos-2 cell line (Supporting Information Figure S5a), and the EC_{50} values for the PTH receptor-mediated cAMP production were determined from the dose−response curves (Table 2).

Upon incubation of conjugates in the concentration range of 1.225 nM−80 μM with Saos-2 cells, none of the fusion peptides gave rise to EC_{50} values comparable to those of expressed unconjugated PTH(1−34) (0.19 ± 0.13 μM) or of a sample of synthetic PTH(1−34) (0.11 ± 0.15 μM) (Supporting Information Figure S5b) included as a reference. Conjugation of Tat to PTH(1−34) overall affected the affinity toward the

DOI: 10.1021/bc5005763
Bioconjugate Chem. 2015, 26, 477−488

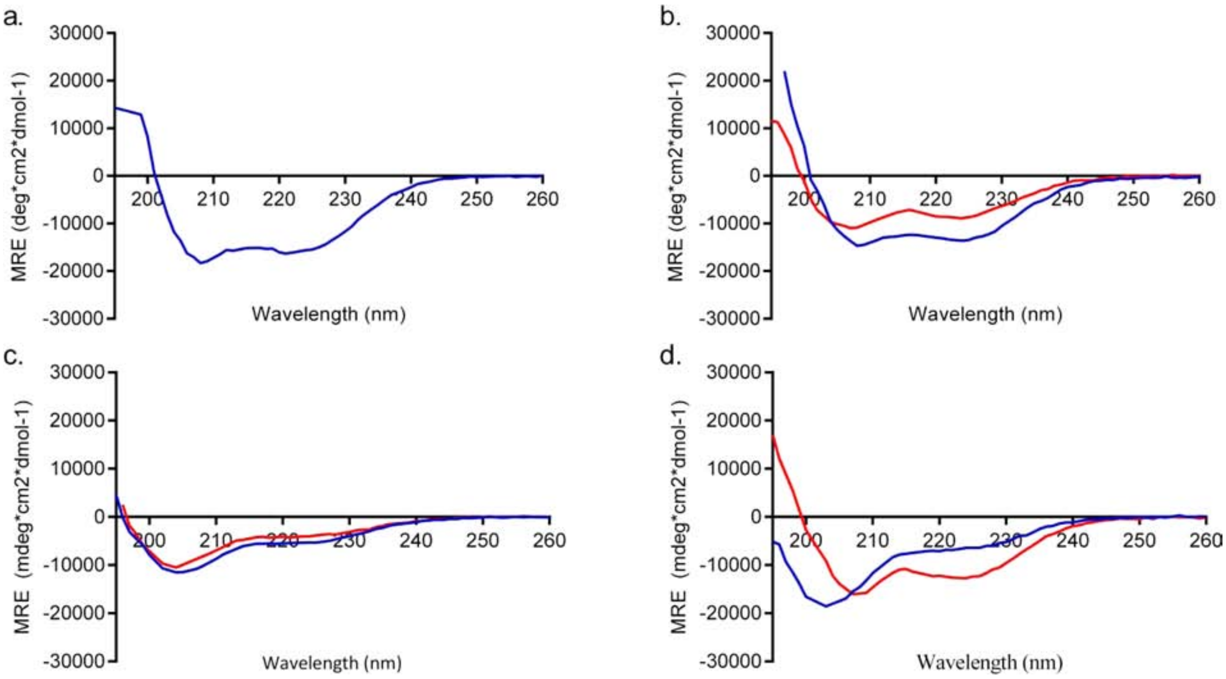

Figure 4. Circular dichroism spectra of CPP-conjugated PTH(1−34) in the presence of 1 mM POPC:POPG (molar ratio 80:20) liposomes corresponding to a 1:100 peptide to lipid ratio. (a) PTH(1−34)-penetratin (blue), (b) Tat-PTH(1−34) (red) and PTH(1−34)-Tat (blue), (c) VP22-PTH(1−34) (red) and PTH(1−34)-VP22 (blue), (d) R9-PTH(1−34) (red) and PTH(1−34)-R9 (blue). All spectra were recorded at a conjugate concentration of 10 μM.

Table 2. EC_{50} Values Obtained after Incubation of Saos-2 Cells with CPP-PTH(1-34) Fusion Peptides[a]

	EC_{50} (μM)	
CPP	CPP-PTH(1−34)	PTH(1−34)-CPP
Penetratin	n.a.	10.76 ± 1.55
Tat	1.58 ± 1.32	4.98 ± 1.30
VP22	14.66 ± 1.63	23.50 ± 1.67
R9	22.59 ± 2.11	6.65 ± 1.25

[a]Data are presented as mean ± SEM (n = 3).

receptor the least, and only Tat-PTH(1−34) was able to elicit an effect comparable to that of unconjugated PTH(1−34) within the range of concentrations tested. Interestingly, for Tat and VP22 C-terminal conjugation to PTH(1−34) led to lower potencies as compared to the corresponding N-terminal conjugation, whereas the opposite trend was found for conjugation of R9 to PTH(1−34).

None of the CPP-Conjugated PTH(1−34) Fusion Peptides Induced an in Vitro Immune Response. When employing bacterial expression of peptides or proteins for potential therapeutic use, the risk of contamination by endotoxins must be taken into consideration in order to decrease the risk of severe side effects as a result of, e.g., an immune response.[22] Further, the presence of endotoxins might influence the membrane permeation studied in vitro. Hence, the expressed PTH(1−34) and CPP-conjugated PTH(1−34) fusion peptides were tested for a possible immunogenic response using a dendritic cell (DC) maturation assay and a Toll-like receptor (TLR) assay. The native expressed PTH(1−34) showed some immunogenic response, as it gave rise to an up-regulation of maturation markers on murine bone marrow-derived dendritic cells (BMDCs) (Figure 5a) and gave rise to activation of human Toll-like receptor (hTLR) hTLR4 on hTLR4 reporter cells (Figure 5b).

Thus, the expressed PTH(1−34) may be contaminated by trace amounts of endotoxins during its production, whereas none of the CPP-conjugated PTH(1−34) fusion peptides or the synthetic sample of PTH(1−34) resulted in positive responses in any of the immunogenicity assays in the range of concentrations tested (0.15−15 μM) (Figure 5 and Supporting Information Figure S6). This may be explained by the higher polarity of the fusion peptides most likely allows for the complete removal of endoxin contaminants during the HPLC purification step.

Transepithelial Permeation Is Dependent on the Terminal Positioning of the CPP. The CPP-conjugated PTH(1−34) fusion peptides were evaluated for their ability to permeate an intestinal epithelium in vitro. In general, N-terminal CPP conjugation to PTH(1−34) resulted in fusion peptides with a significantly increased permeation as compared to C-terminal CPP conjugation to PTH(1−34) (Figure 5a−c). This trend is further reflected in the calculated apparent permeability coefficients (P_{app}) (Table 3).

Both N- and C-terminal R9-conjugation to PTH(1−34) (Figure 6c) resulted in the highest amount of transported fusion peptide as compared to conjugation of Tat (Figure 6a), VP22 (Figure 6b), and penetratin to PTH(1−34) (Table 3). Moreover, only the R9-conjugates and the N-terminal Tat- and VP22-PTH(1−34) were able to permeate the Caco-2 monolayer in amounts comparable to unconjugated PTH(1−34) co-administered with the individual CPPs in a molar ratio of 1:1 (Table 3). In general, N-terminal conjugation of the CPPs to PTH(1−34) increased the permeation of the fusion peptide significantly as compared to C-terminal conjugation, but only N-terminal R9-conjugation to PTH(1−34) gave rise to increased transepithelial transport as compared to the

DOI: 10.1021/bc5005763
Bioconjugate Chem. 2015, 26, 477−488

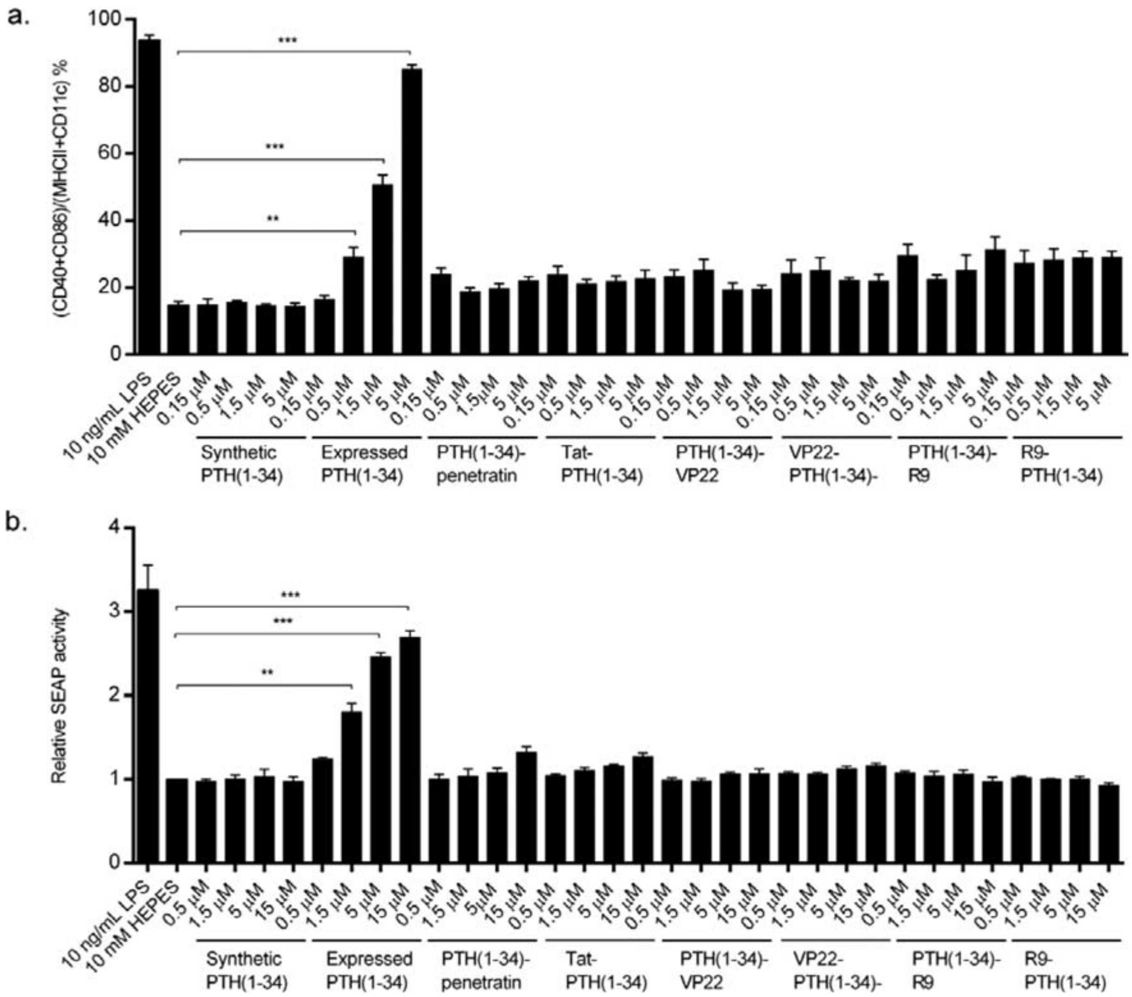

Figure 5. In vitro immune responses obtained by fluorescence-activated cell sorting (FACS) analysis of expression levels of maturation markers CD40 and CD86 on GM-CSF-differentiated murine bone marrow-derived DCs after incubation with 0.15−15 μM synthetic PTH(1−34), expressed PTH(1−34) or the CPP-PTH(1−34) fusion peptides (a) or analysis of human TLR4 activation on HEK-Blue-hTLR4 cells after incubation with 0.5−15 μM synthetic PTH(1−34), expressed PTH(1−34) or the CPP-PTH(1−34) fusion peptides (b). LPS (10 ng/mL) is included as positive control, while 1 mM HEPES buffer is included as negative control. Data are presented as mean ± SEM (n = 4). Levels of significance are ***: p < 0.001 and **: p < 0.01.

Table 3. Apparent Permeability Coefficient (P_{app}) Determined after Application of CPP-PTH(1−34) Fusion Peptides (40 μM) or Similar Total Concentrations of PTH(1−34) Co-administered with Individual CPPs (Molar Ratio 1:1) across Caco-2 Cell Monolayers[a]

	P_{app} (10^{-9} cm/s)		
CPP	CPP-PTH(1−34)	PTH(1−34)-CPP	Co-administration of CPP and PTH(1−34)
Penetratin	n.a.	1.62 ± 0.47	3.61 ± 0.88
Tat	2.56 ± 0.46	1.73 ± 0.40	3.60 ± 0.36
VP22	2.23 ± 0.66	0.32 ± 0.12	2.63 ± 0.94
R9	6.03 ± 3.18	3.42 ± 1.02	2.66 ± 0.74

[a]Data are based on calculations to the end-point and presented as mean ± SEM (n = 6).

uncoupled PTH(1−34) control (P_{app} = (4.64 ± 1.85) × 10^{-9} cm/s). Due to a possible contamination by endotoxins during the isolation of expressed PTH(1−34) (Figure 5), the synthetic PTH(1−34) was included in the permeation studies as a reference and when co-administered with the CPPs, in order to avoid false positive effects when evaluating the viability of the Caco-2 cells and the integrity of the cell monolayer (Figure 7).

R9-Coupled PTH(1−34) Fusion Peptides Decrease Cellular Viability. Following each permeation experiment, the cellular viability was assessed in order to determine whether the permeation of the CPP-conjugated PTH(1−34) fusion peptides was associated with decreased cell viability. No decrease in cell viability was observed upon exposure to penetratin-, Tat-, or VP22-conjugated PTH(1−34), while a significant decrease in cell viability was observed for the R9-conjugated fusion peptides, with the C-terminally R9-modified PTH(1−34) being the most toxic to the cells (Figure 7a). In comparison, co-administration of PTH(1−34) with the CPPs in a molar 1:1 ratio did not affect cell viability (Figure 7c). The observations indicated a tendency toward C-terminally CPP-

DOI: 10.1021/bc5005763
Bioconjugate Chem. 2015, 26, 477−488

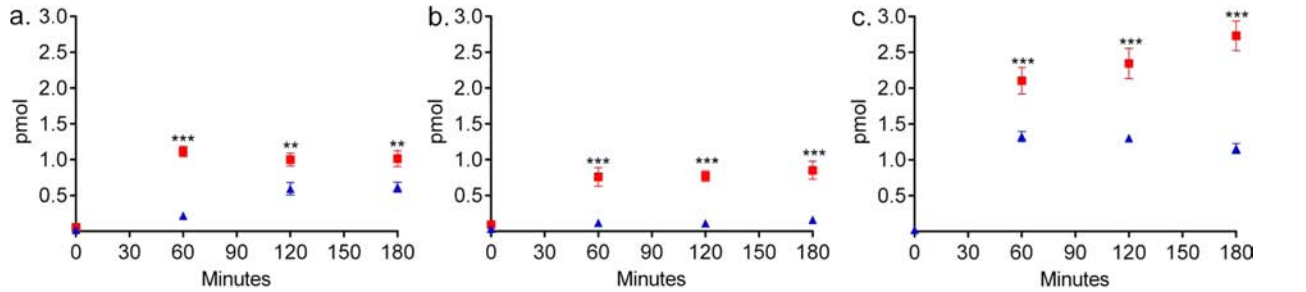

Figure 6. Permeation of PTH(1−34) after application of 40 μM Tat-conjugated PTH(1−34) (a), 40 μM VP22-conjugated PTH(1−34) (b), or 40 μM R9-conjugated PTH(1−34) (c) across Caco-2 cell monolayers. Red: N-terminal CPP. Blue: C-terminal CPP. Data are presented as mean ± SEM (n = 6). Levels of significance are ***: p < 0.001 and **: p < 0.01.

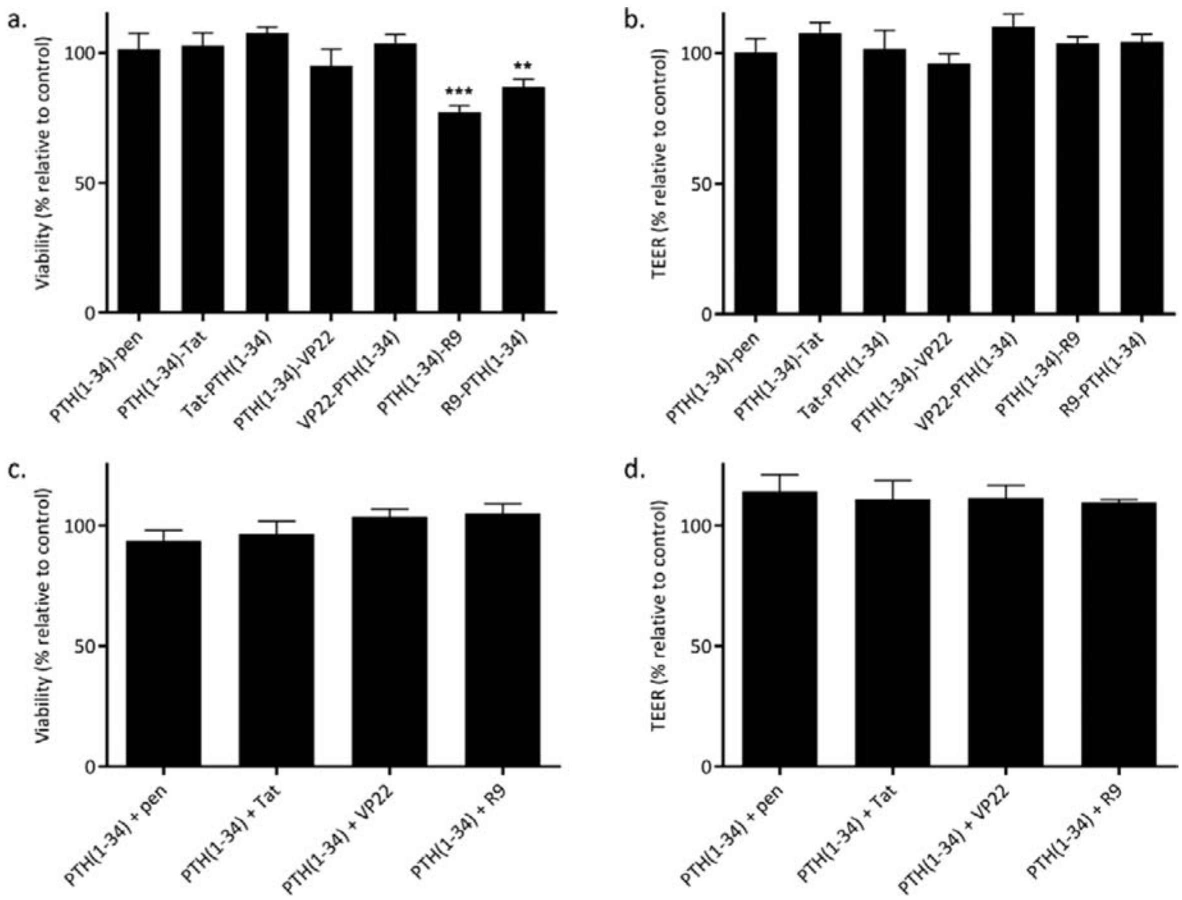

Figure 7. Cell viability of Caco-2 cells in monolayers after a 3 h permeation study applying 40 μM CPP-conjugated fusion peptide (a) or similar concentrations of PTH(1−34) co-administered with penetratin, Tat, VP22, or R9 (c) and the relative TEER measured after the experiment (b, d). Results are shown as % relative to control (10 mM HEPES in HBSS pH 7.4) ± SEM (n = 6). Levels of significance are ***: p < 0.001 and **: p < 0.01 compared to control.

conjugated PTH(1−34) fusion peptides being slightly more toxic to Caco-2 cells in monolayers than the N-terminally CPP-conjugated analogues. However, despite the reduced cell viability observed after exposure to the R9-conjugated PTH(1−34), no effect on the epithelial integrity of the monolayer was observed upon application of any of the fusion peptides (Figure 7b) or as a result of incubation with PTH(1−34) co-administered with the CPPs (Figure 7d).

■ DISCUSSION

Major progress within the biotechnological area has enabled large-scale expression and purification of recombinant peptides and proteins with a high degree of purity, which makes it possible to establish a tightly controlled high-throughput production of, e.g., dual-function fusion peptides and proteins for therapeutic use. In the present study, CPP-conjugated PTH(1−34) fusion peptides were successfully produced in *E. coli* and purified from IBs in order to study the effect of CPP conjugation on the characteristics of a therapeutic peptide. Thus, the effect of direct conjugation of a CPP to the N- or C-terminus of the therapeutically relevant PTH(1−34) was investigated with respect to structural characteristics, potency, immunogenicity induction, ability to permeate epithelial monolayers, and safety profile.

When producing recombinant peptides and proteins, soluble expression is usually desired in order to avoid time-consuming

DOI: 10.1021/bc5005763
Bioconjugate Chem. 2015, 26, 477−488

and complicated solubilization and refolding steps of otherwise insoluble IBs. Overexpression, however, of eukaryotic proteins in *E. coli*, being the most widely used prokaryotic host, often leads to the formation of IBs,[23,24] as was also the case with the expression of PTH(1−34) and of four out of seven of the CPP-conjugated PTH(1−34) fusion peptides produced in the present project. On the other hand, expression of peptides and small proteins into IBs has several advantages: (i) IBs are often expressed in high concentrations, (ii) IBs almost exclusively contain the expressed peptide or protein of interest,[25] (iii) IBs are readily isolated by centrifugation,[26] and (iv) the insoluble aggregates possibly confer protection against enzymatic degradation.[25] For the production of both PTH(1−34) and the CPP-conjugated PTH(1−34) fusion peptides, the expression was therefore deliberately forced into IB production, and a protocol for the solubilization and purification from these was developed (Figure 1, top), and by this method PTH(1−34) and the CPP-conjugated PTH(1−34) fusion peptides were successfully isolated with a high purity (Figure 2).

CD spectra of PTH(1−34) revealed a poorly defined secondary structure in an aqueous buffer, while it adopted an α-helical structure in the presence of both 20% (v/v) aqueous TFE and POPC:POPG liposomes (Figure 3) similarly to previously reported data.[27−29] Moreover, it was shown that the potency of the expressed PTH(1−34) was comparable to the potency of a synthetic PTH(1−34) (Supporting Information Figure S5b). Thus, the newly developed protocol for the purification from IBs is highly suitable for the purification of bioactive molecules. However, the risk of contamination by endotoxins when using a prokaryotic expression host must always be considered, as such trace contaminations may elicit undesired immunogenic responses, which in the present study was actually observed to be the case for the expressed PTH(1−34) (Figure 5).

Regarding the CPP-conjugated PTH(1−34) fusion peptides, CD spectra revealed that the degree of folding into an α-helical secondary structure generally increased in the presence of 20% (v/v) aqueous TFE (Supporting Information Figure S3b) as also observed for PTH(1−34) (Figure 3). In the presence of POPC:POPG liposomes, only C-terminally penetratin- and Tat-conjugated PTH(1−34) and N-terminally R9-conjugated PTH(1−34) were able to fold into an α-helical structure similar to the expressed PTH(1−34) (Figure 4a,b,d). Hence, both the specific sequence and the specific positioning of the CPP influence the overall secondary structure of the CPP-conjugated PTH(1−34) fusion peptide. NMR spectroscopy studies have shown that addition of TFE to solutions of PTH(1−34) stabilizes α-helical structures both at the N- and C-terminus,[27] of which the former positively affects the pharmacological activity in vivo.[18] In the present study, the ability to adopt an α-helical structure in the presence of POPC:POPG lipid membranes did not generally correlate with an increased potency of the CPP-conjugated PTH(1−34) fusion peptides as determined in vitro (Table 2), since only the N-terminally Tat-conjugated PTH(1−34) was capable of eliciting a maximum response comparable to that of the expressed PTH(1−34) reference within the range of concentrations tested (Supporting Information Figure S5a). Hence, there is no clear correlation between the ability to adopt an α-helical structure and the potency in vitro of the CPP-conjugated PTH(1−34) fusion peptides.

Tat-PTH(1−34) was found to be the most potent of the CPP-conjugated PTH(1−34) fusion peptides, while both the VP22-conjugates and the R9-PTH(1−34) were less potent (Table 2). VP22 with its 34 residues is the longest of the CPPs employed. Consequently, there may be an upper limit for the length of the CPP sequence conjugated to PTH(1−34) that allows for retaining the potency of the resulting fusion peptide. A short CPP seems, however, not to be the sole determinant for maintaining potency of the therapeutic peptide when conjugated to PTH(1−34), since the Tat-conjugated PTH(1−34) fusion peptides were significantly more potent than the R9-conjugated PTH(1−34) analogue, despite a similar sequence length (i.e., 11 versus 9 residues). Hence, the specific sequence of the CPP also affects potency of the CPP-conjugated PTH(1−34) fusion peptide.

The pharmacologically active PTH(1−34) is composed of two functionally relevant regions interconnected by a flexible linker region.[27] The C-terminal residues 14−34 are involved in receptor binding,[30] whereas the N-terminus is crucial for receptor activation.[31] Although conjugation of a CPP to the C-terminus of PTH(1−34) will keep the N-terminus available for receptor activation, it did not seem to be a general approach for retaining potency of the resulting conjugate (Table 2), supporting the hypothesis that the specific length and amino acid composition of the CPP are both determinants for the overall potency of the fusion peptide. Nevertheless, a clear difference in potency of both the Tat- and the R9-conjugated PTH(1−34) fusion peptides due to N- vs C-terminal attachment was observed. Thus, the specific positioning of the CPP plays a role in the potency of the individual Tat- or R9-conjugated PTH(1−34) fusion peptides, but whether N- or C-terminal conjugation to PTH(1−34) is preferred with respect to achieving the most potent fusion peptide is dependent on the specific CPP.

The CPP-conjugated PTH(1−34) fusion peptides were evaluated for their ability to permeate the Caco-2 cell monolayers (Figure 6). N-Terminal conjugation of the CPPs to PTH(1−34) significantly increased the transepithelial permeation as compared to that seen for the corresponding C-terminally CPP-conjugated PTH(1−34) fusion peptides. Thus, N-terminal R9-conjugation conferred the highest increase in permeation for the PTH(1−34) conjugate (approximately 2- to 3-fold as compared to C-terminally conjugated Tat or VP22; Table 3). With regard to the C-terminally conjugated fusion peptides, R9 was superior in increasing the transepithelial PTH(1−34) permeation as compared to C-terminally conjugated penetratin, Tat and VP22. Exposure to the R9-PTH(1−34) fusion peptides was, however, associated with a decrease in cell viability, with the C-terminally R9-conjugated PTH(1−34) being slightly more toxic than the N-terminal analogues (Figure 7a). This slight cytotoxic effect was, however, not associated with a decrease in the epithelial integrity (Figure 7b). The decrease in cell viability is most likely caused by irreversible membrane perturbations mediated by the high number of guanidinium groups present in the R9 sequence, an effect previously found to be correlated with an increased number of arginine residues in CPP sequences.[32,33] Nevertheless, no decrease in cell viability was observed as a result of co-administration of R9 with PTH(1−34) in a 1:1 molar ratio corresponding to the concentrations of the R9-coupled PTH(1−34) fusion peptides (Figure 7c). A plausible explanation of this finding is that complexes are formed by the physical mixing of PTH(1−34) with the CPPs,

DOI: 10.1021/bc5005763
Bioconjugate Chem. 2015, 26, 477−488

which shield some of the arginine residues of R9, hence protecting the plasma membrane against an excessively high local concentration of guanidinium groups that might lead to a decreased cell viability. Also, conjugation of R9 to PTH(1−34) may result in longitudinal amphipathicity,[34] thereby causing membrane damage thus explaining the negative effect on viability exerted by the fusion peptides when compared to PTH(1−34) coadministered with R9.

Except for the R9-conjugated PTH(1−34) fusion peptides, the co-administration approach generally resulted in a slightly higher amount of transported PTH(1−34) as compared to the covalent conjugation approach, with penetratin and Tat being superior to both VP22 and R9. Therefore, the inherent proximity of the CPP to the therapeutic peptide as a result of direct conjugation seems not to be an advantage when employing CPPs as transepithelial permeation enhancers for the delivery of a therapeutic peptide such as PTH(1−34). An explanation could be that a possible formation of complexes between the CPP and PTH(1−34) may confer some protection against enzymatic degradation of the CPP, thereby maintaining an intact and functional CPP moiety.

CONCLUSIONS

In conclusion, the present study reveals that it is possible to express and purify a series of CPP-conjugated PTH(1−34) fusion peptides from IBs, and that these samples were nonimmunogenic. While the CPP conjugation to PTH(1−34) generally maintained the propensity to fold into an α-helical structure in the presence of lipid bilayers, the conjugation to a CPP led to a generally decreased potency without any clear dependency on whether conjugation was at the N- or C-terminus of PTH(1−34). By contrast, transepithelial permeation of the compounds revealed that introduction of a CPP at the N-terminus of PTH(1−34) gave rise to increased permeation across Caco-2 monolayers in comparison to C-terminally CPP-conjugated PTH(1−34). In particular R9-modified PTH(1−34) permeated well across the epithelium, and although this was associated with a slight decrease in cell viability, no negative effect on the epithelial membrane integrity could be detected. Further studies are needed to evaluate the potential benefit of conjugation of CPPs to PTH(1−34), with the present study demonstrating the need for more advanced conjugation designs than simple terminal positioning of the CPP.

EXPERIMENTAL PROCEDURES

Materials. Primers were designed using VectorNTI 11 software (Life Technologies, Naerum, Denmark) (Supporting Information Table S1) and cDNA encoding CPP-modified PTH(1−34) fusion peptides were obtained as synthetic genes from GeneArt (Life Technologies, Naerum, Denmark). All enzymes were obtained from New England Biolab (Ipswich, MA, USA). For cloning *E. coli*, Mach1 cells (Life Technologies, Naerum, Denmark) were employed and antibiotics (Sigma-Aldrich, Buchs, Switzerland) were used in the following concentrations: kanamycin 50 μg/mL, chloramphenicol 34 μg/mL. All cells were grown in Terrific Broth (TB) medium (tryptone 12.0 g/L, yeast extract 24.0 g/L, K_2HPO_4 9.4 g/L, KH_2PO_4 2.2 g/L) containing 8 g/L glycerol as a carbon source. For inhibition of enzymatic activity during protein purification Complete Mini EDTA-free protease inhibitor tablets were used (Roche, Hvidovre, Denmark).

Rink amide resin and coupling reagents for solid-phase peptide synthesis of penetratin, Tat and nonaarginine (R9) were purchased from Fluka (Buchs, Switzerland). All amino acid building blocks as well as other solvents and chemicals for peptide synthesis were purchased from Iris Biotech (Merktredwitz, Germany). PTH(1−34) and VP22 were obtained as synthesized peptides from BACHEM (Bubendorf, Schwitzerland) and Selleckchem (Munich, Germany), respectively. All other materials were obtained from Sigma-Aldrich (Buchs, Switzerland).

Cloning and Expression. Generation of expression constructs: Proteins were expressed using the plasmid pNIC28-Bsa4 (GenBank ID: EF198106) containing an N-terminal hexahistidine tag followed by a TEV protease site (ENLYFQ*SS), two *Bsa*I sites for ligase-independent cloning (LIC) and a *sacB* fragment, which allows for negative selection on sucrose. Sequences of interest were cloned into the vector using LIC as previously described.[35] Briefly, DNA sequences encoding CPP-modified PTH(1−34) fusion peptides of interest and flanked by LIC sites were amplified by PCR, digested with T4 DNA polymerase, and cloned into pNIC28-Bsa4. Successfully transformed vectors were selected on Luria Broth (LB) agar plates containing 50 μg/mL kanamycin and 5% (w/v) sucrose before purification using a Miniprep kit (Macherey-Nagel, Germany). Sequences were verified using an ABI Prism 3700 Analyzer (Life Technologies, Naerum, Denmark) before being transformed into Rosetta expression strains (Millipore, Schwalbach, Germany), which were kept as glycerol stocks for long-term storage at −80 °C.

Protein expression as inclusion bodies: Transformed clones was inoculated in TB medium supplemented with kanamycin (50 μg/mL) and incubated overnight at 37 °C and 180 rpm. Seven mL overnight culture was transferred to 700 mL TB supplemented with kanamycin (50 μg/mL) in 2 L flasks and incubated at 37 °C and 180 rpm until OD600 reached 1.5. Protein expression was induced by 0.5 mM isopropyl β-D-1-thiogalactopyranoside (IPTG) and continued overnight at 37 °C and 180 rpm.

Peptide Purification. The overnight culture was centrifuged at 3512 G using a FIBERLite F8−6 × 1000y rotor (Thermo Fisher Scientific, Waltham, MA, USA) in a Sorvall Evolution RC centrifuge (Thermo Fischer Scientific, Waltham, MA, USA) for 10 min at 4 °C, and the pellet was dissolved in lysis buffer (50 mM Tris-HCl, 100 mM NaCl, 10 mM imidazole, 0.5 mM TCEP, 1 Complete Mini EDTA-free protease inhibitor, 50 U/mL benzonase; pH 8) at 4 °C before homogenization using an Emulsiflex-D20B high pressure homogenizer (Avestin, Ottawa, Ontario, Canada). IBs were collected by centrifugation at 18 566 G using a FIBERLite F14−6 × 250y rotor (Thermo Fischer Scientific, Waltham, MA, USA) in a Heraeus X3R Multifuge (Thermo Fischer Scientific, Waltham, MA, USA) for 30 min at 4 °C, and then washed in ice-cold buffer (50 mM Tris-HCl, 100 mM NaCl, 0.5%(v/v) Triton X-100; pH 8) before centrifugation and solubilization (50 mM Tris-HCl, 300 mM NaCl, 10 mM imidazole, 6 M guanidinium chloride; pH 8) overnight at room temperature. Solubilized IBs were isolated by centrifugation at 18,566 G using a FIBERLite F14−6 × 250y rotor (Thermo Fischer Scientific, Waltham, MA, USA) in a Heraeus X3R Multifuge (Thermo Fischer Scientific, Waltham, MA, USA) for 1.5 h at room temperature before filtration through a 0.22 μm PES bottle top filter (MidSci, St. Louis, MO, USA) and purification using a HiTrap Chelating column (GE Healthcare, Broendby,

DOI: 10.1021/bc5005763
Bioconjugate Chem. 2015, 26, 477−488

Denmark) coupled to an ÄKTA Xpress system (GE Healthcare, Broendby, Denmark) at room temperature. The column was equilibrated with 10 column volumes (CV) binding buffer (50 mM Tris-HCl, 300 mM NaCl, 10 mM imidazole, 0.5 mM tris(2-carboxyethyl)phophine (TCEP), 6 M urea; pH 8) before sample loading followed by wash in 10 CV wash buffer (50 mM Tris-HCl, 300 mM NaCl, 30 mM imidazole, 0.5 mM TCEP, 6 M urea; pH 8). Peptides were eluted with elution buffer (50 mM Tris-HCl, 300 mM NaCl, 300 mM imidazole, 0.5 mM TCEP, 6 M urea; pH 8) in 2 mL fractions based on the absorbance at 280 nm. Peptide fractions were lyophilized in a Christ Alpha 2−4 LD plus freeze−dryer (Martin Christ Gefriertrocknungsanlagen, Osterode am Harz, Germany) before they were dissolved in 10 mM HEPES pH 7.4 added 0.05% (v/v) trifluoroacetic acid (TFA) and further purified by RP-HPLC (150 × 4.6 mm Phenomenex Jupiter C18 column, 3 μm) by applying a linear gradient of eluent B (acetonitrile (MeCN), 0.05%(v/v) TFA) in eluent A (5% (v/v) MeCN, 0.05% (v/v) TFA, Milli-Q water) increasing from 0% to 100% over 100 min at room temperature. Fractions containing eluted peptide identified based on the absorbance at 280 nm were lyophilized and the N-terminal histidine-tag was cleaved off by incubation with the TEV protease (1 mol TEV to 100 mol target peptide) in TEV buffer (10 mM HEPES, 0.5 mM TCEP; pH 7.4) overnight at 4 °C. Target peptides were separated from the histidine-tag by RP-HPLC using the same method as described above. Eluted peptide fractions were lyophilized, dissolved in 10 mM HEPES pH 7.4, identified on an Instant Blue Coomassie stained (Expedeon, Cambridgeshire, UK) NuPAGE 4−12% Bis-Tris SDS-PAGE (Life Technologies, Naerum, Denmark), and molecular weights verified by LC-HRMS using a Bruker MicrOTOF-Q II Quadropol MS detector (Bruker, Coventry, UK) and stored at −80 °C until further use.

Peptide Synthesis. Synthesis of penetratin, Tat, and R9 was carried out as previously described[20] by Fmoc solid-phase peptide synthesis (SPPS) using a MW-assisted automated CEM Liberty synthesizer (CEM, Matthews, NC, USA). The peptides were purified by preparative RP-HPLC (250 × 21.2 mm Phenomenex Luna C18(2) column, particle size: 5 μm). A linear gradient of eluent B (MeCN−water 95:5 with 0.1% (v/v) TFA) in eluent A (MeCN−water 5:95 with 0.1% (v/v) TFA) increasing from 0% to 45% over 25 min was applied at room temperature. The purity of the peptides (>95%) was confirmed by analytical RP-HPLC (150 × 4.6 mm Phenomenex Luna C18(2) column, particle size: 3 μm) with UV detection at 220 nm by using a gradient from 0% to 60% of B over 30 min, while the molecular identity was confirmed by LC-HRMS using a Bruker MicrOTOF-Q II Quadropol MS detector. The peptides were lyophilized and stored at −18 °C until further use. The synthesized peptides are listed in Table 2.

Immunogenicity testing. *TLR Activation Assay.* Human Toll Like Receptor reporter cell lines (HEK-Blue-hTLRNull1, -hTLR2, -hTLR3, -hTLR4, and -hTLR9 reporter cells) were cultured according to the manufacturer's directions (Invitrogen, Toulouse, France). 25 000 HEK-Blue-hTLRNull1, -hTLR2, or -hTLR3 reporter cells; 12 500 HEK-Blue-hTLR4 cells; or 40 000 HEK-Blue-hTLR9 cells were stimulated with 0.5, 1.5, 5, or 15 μM PTH(1−34) or PTH(1−34)-CPP fusion peptides in a total volume of 100 μL for 20 h at 37 °C in a humidified CO_2 incubator. As positive controls, the following agonists (Invitrogen, Toulouse, France) were used: Pam3SCK (100 ng/mL) for TLR2, LPS-EK (10 ng/mL) for TLR4, ODN2006 (10 μg/mL) for TLR9, Poly(I:C) (5 ug/mL) for TLR3, and TNF-α (100 ng/mL) for TLRNull. To detect secreted reporter protein alkaline phosphatase, 20 μL supernatant was added to 180 μL of QUANTI-Blue substrate (Invitrogen, Toulouse, France) and incubated for 1 h at 37 °C in a humidified CO_2 incubator. Levels of secreted alkaline phosphatase (SEAP) were determined using a Biorad microplate reader at 650 nm. Relative alkaline phosphatase levels were defined as sample level divided by water control level.

DC Maturation Assay. Dendritic cells were obtained as previously described by Lutz et al.[36] Briefly, bone marrow was flushed from femurs and tibia of CB6F1/CrL mice (6−8 weeks) before they were flushed with culture medium (20 ng/mL murine rGM-CSF (Cytogen, The Netherlands) in Iscove's Modified Dulbecco's Medium supplemented with 5% (v/v) fetal bovine serum (Lonza, Verviers, Belgium), 50 μM 2-mercaptoethanol (Sigma-Aldrich, St. Louis, MO, USA), penicillin, and streptomycin (adapted from Lutz et al.).[36] 450 000 cells were seeded in 1 mL per well in a 12-well plate expanded in culture medium. On day 2, the growth medium volume was doubled, and on day 5, additional 20 ng/mL rGM-CSF was added. On day 7, BMDCs were stimulated with PBS (1:1000), LPS (10 ng/mL), or 1 of the 8 PTH(1−34) test solutions (5, 1.5, 0.5, or 0.15 μM) for 16 h at 37 °C in a humidified CO_2 incubator. Staining of surface markers with the indicated antibodies was performed in the presence of Fc block (2.4G2) for 30 min on ice. Anti-CD11c (N418) and -I-Ad/I-Ed (M5/114) were purchased from eBioscience (San Diego, CA, USA) and anti-CD40 (3/23) and -CD86 (GL1) were obtained from BD Biosciences (Breda, The Netherlands). Samples were measured on a FACSCantoII (BD Biosciences, San Jose, CA, USA) and analyzed with *FlowJo* software (Ashland, OR, USA).

Liposome Preparation. Anionic unilamellar liposomes (POPC:POPG, 80:20 molar ratio) were prepared for circular dichroism (CD) spectroscopy by the thin film method as previously described.[37] Briefly, dry lipid films were formed in round-bottom flasks under vacuum overnight before they were hydrated for 1 h at room temperature, with vigorous agitation every 10 min, in a buffer containing 10 mM HEPES and 150 mM KCl (pH 7.4) to obtain a final lipid concentration of 20 mM. Upon annealing for 1 h, vesicles were extruded (Lipex Biomembranes Extruder, Vancouver, BC, Canada) 10 times through two stacked polycarbonate filters with 100 nm pore size (Whatman, Herlev, Denmark). For all batches used, the expected vesicle size and polydispersity index (PDI) were verified by dynamic light scattering (DLS) at 25 °C using a Zetasizer Nano ZS (Malvern Optics Instruments, Worcestershire, UK) equipped with a 633 nm laser.

Secondary Structure Determination. CD spectra of the CPP-modified PTH(1−34) fusion peptides or CPPs alone, in the presence of 20%(v/v) 2,2,2-trifluoroethanol (TFE), or mixed with POPC:POPG liposomes at a fixed peptide to lipid ratio of 1:100 were measured in the range of 180−260 nm on a JASCO spectrophotometer (Easton, MD, USA) using a 1 mm cuvette (Hellma Analytics, Müllheim, Germany). Measurements were performed at 20 °C with 10 μM PTH(1−34), 10 μM CPP-modified PTH(1−34), or 20 μM CPP mixed with 20 μM PTH(1−34) dissolved in Milli-Q water. All spectra were background corrected, transformed into mean residue ellipticity (MRE), and represent an average of 10 scans.

Cell Culture Models. For potency assessment, Saos-2 cells were obtained from American Type Culture Collection (ATCC, Manassas, VA, USA) and maintained in McCoy's 5A

DOI: 10.1021/bc5005763
Bioconjugate Chem. 2015, 26, 477−488

medium (Sigma-Aldrich, Broendby, Denmark) supplemented with 90 U/mL penicillin, 90 μg/mL streptomycin, 2 mM L-glutamine, 0.1 mM nonessential amino acids, and 10% (v/v) fetal calf serum (FCS) (Thermo Fischer Scientific, Slangerup, Denmark). Cells were grown in 5% CO_2 at 37 °C and detached from the culturing flasks at 80% confluence by trypsin-EDTA treatment before being subcultured at a ratio of 1:5 once a week. Before experimental use, 5.0×10^4 cells/well were seeded at in 96-microtiter plates and cultured for 2 days.

For the permeability and viability studies, Caco-2 cells were obtained from American Type Cell Cultures (ATCC, Manassas, VA, USA) and maintained in Dulbecco's Modified Eagle Medium (DMEM) (Sigma-Aldrich, Broendby, Denmark) supplemented with 90 U/mL penicillin, 90 μg/mL streptomycin, 2 mM L-glutamine, 0.1 mM nonessential amino acids, and 10% (v/v) fetal calf serum (FCS) (Thermo Fischer Scientific, Slangerup, Denmark). Cells were grown in 5% CO_2 at 37 °C and detached from the culturing flasks at 80% confluence by trypsin-EDTA treatment before being subcultured at a ratio of 1:5 twice a week. For experimental use 1.0×10^5 cells were grown on polycarbonate membrane inserts (diameter: 12 mm, area: 1.13 cm^2, pore size 0.4 μm) (Corning Costar, Costar, NY, USA) in a 12-well Transwell plate (Corning Costar, Costar, NY, USA) for 20 days.

Potency Assessment. Saos-2 cells were washed once with phosphate buffered saline (PBS) and incubated with PTH(1−34) and CPP-conjugated PTH(1−34) fusion peptides dissolved in PBS containing 0.1 mM 4-(3-butoxy-4-methoxybenzyl)-imidazolidin-2-one) (Sigma-Aldrich, Broendby, Denmark) and 0.5 mM 3-isobutyl-1-methylxanthine (Sigma-Aldrich, Broendby, Denmark) for 1 h at 37 °C with peptide concentrations ranging from 1.225 nM−80 μM. cAMP levels were determined using the bioluminescent cAMP-Glo assay (Promega, Madison, WI, USA) according to the procedure supplied by the manufacturer. Luminescence was measured on a FLUOstar OPTIMA plate reader (BMG Labtech, Offenburg, Germany) for quantification.

In Vitro Permeation Studies. Test samples containing 40 μM CPP-PTH(1−34) fusion peptide or corresponding concentrations of commercially obtained PTH(1−34) mixed with either penetratin, Tat, VP22, or R9 were prepared in Hanks Balanced Salt Solution (HBSS) (Invitrogen, Naerum, Denmark) supplemented with 10 mM HEPES (Applichem, Darmstadt, Germany), and adjusted to pH 7.4 (hHBSS). ^{3}H-mannitol (1 μCi/mL in hHBSS) was included as a control of the integrity of the Caco-2 cell monolayer.

Before initiation of the experiment, the monolayer was washed with 2 × 1 mL hHBSS and subsequently left to equilibrate to room temperature in the last rinsing volume prior to measuring the transepithelial electrical resistance (TEER) followed by equilibration to 37 °C. The hHBSS was removed from the apical and basolateral compartments and the experiment initiated by the addition of 500 μL of the respective test samples before the filter inserts were transferred to new 12-well plates prefilled with 1 mL hHBSS. From wells containing ^{3}H-mannitol, 100 μL samples were withdrawn from the basolateral compartment at time points 0, 30, 60, 90, 120, 150, and 180 min and immediately mixed with 2 mL Ultima Gold (PerkinElmer, Waltham, MA, USA) before being subjected to analysis using a scintillation counter (Packard Tri-Carb 2100 TR, Canberra, Dreieich, Germany). From the wells containing the test samples, 100 μL samples were withdrawn at time points 0, 60, 120, and 180 min and kept on ice until quantification of the amount of permeated PTH(1−34) employing an EIA kit (BACHEM, Bubendorf, Schwitzerland) as described by the manufacturer using the absorbance measured at 450 nm on a FLUOstar OPTIMA plate reader (BMG Labtech, Offenburg, Germany) for quantification. Withdrawn samples were immediately replaced with the same volume of receptor medium.

The apparent permeability coefficient (P_{app}) was calculated by using the equation

$$P_{app}(\mathrm{cm/s}) = \mathrm{d}Q/\mathrm{d}t \times 1/(A \times C_0) \quad (1)$$

where dQ/dt is the steady state flux, A (1.13 cm^2) is the area of the Caco-2 cell monolayer, and C_0 is the initial donor concentration.

Viability Assessment. The cellular viability of the Caco-2 cells in the monolayer was determined immediately after each permeability study and assayed using the MTS/PMS assay as previously described.[38] Briefly, the monolayer was incubated with 0.32 mL of a MTS/PMS solution (240 μg/mL MTS, 2.4 μg/mL PMS (Promega, Madison, WI, USA) in hHBSS) for 1.5 h with horizontal shaking (50 rpm, 37 °C). The absorbance of 100 μL samples (n = 2) from each well was subsequently measured at 492 nm on a POLARstar OPTIMA plate reader (BMG Labtech, Offenburg, Germany). The relative viability was calculated by using the equation

$$\begin{aligned} &\text{relative viability (\%)} \\ &\quad = (A_{\text{sample}} - A_{\text{SDS}})/(A_{\text{buffer}} - A_{\text{SDS}}) \times 100\% \end{aligned} \quad (2)$$

where A_{sample} is the absorbance of the samples, A_{SDS} is the absorbance of the negative control (0.2% (w/v) sodium dodecyl sulfate (SDS)) corresponding to 0% cell viability, and A_{buffer} is the absorbance of the positive control that corresponds to 100% cell viability.

Data and Statistical Analysis. Data processing was done in *Microsoft Office Excel 2010* and *GraphPad Prism* v 6 (GraphPad Software, San Diego, CA, USA). Statistical analysis was carried out in *GraphPad Prism* v 6 using t test and one way analysis of variance (ANOVA), and data shown as mean ± standard error of mean (SEM) with n representing the number of replicates. The permeation studies were performed using 3 consecutive passages of cells.

■ ASSOCIATED CONTENT

Supporting Information

Overview of the primers and the plasmid used for cloning, data on soluble expression, CD spectra of the fusion peptides in aqueous buffer and TFE, CD spectra of the CPPs alone, dose−response plots after incubation of fusion peptides with Saos-2 cells, and data on immune response causing TLR2-, TLR3-, or TLR9-activation. This material is available free of charge via the Internet at http://pubs.acs.org.

■ AUTHOR INFORMATION

Corresponding Author

*E-mail: hanne.morck@sund.ku.dk.

Notes

The authors declare no competing financial interest.

■ ACKNOWLEDGMENTS

Senior Technician Maria Læssøe Pedersen and Thara Hussein (Department of Pharmacy, University of Copenhagen) are acknowledged for the cell culturing and PhD Jesper Søborg Bahnsen (Department of Pharmacy, University of Copenhagen) is acknowledged for the synthesis of penetratin. The work was financially supported by the Drug Research Academy (University of Copenhagen), The Danish Agency for Science, Technology & Innovation, and the Novo Nordisk Foundation Center for Protein Research for PhD student Mie Kristensen. Additionally, the research leading to these results has received support from the Innovative Medicines Initiative Joint Undertaking under grant agreement no 115363 resources which are composed of financial contribution from the European Union's Seventh Framework Programme (FP7/2007-2013) and EFPIA companies in kind contribution.

REFERENCES

(1) Kargi, A. Y., and Merriam, G. R. (2013) Diagnosis and treatment of growth hormone deficiency in adults. *Nat. Rev. Endocrinol. 9*, 335−345.

(2) Rozenberg, S., Vandromme, J., and Antoine, C. (2013) Postmenopausal hormone therapy: risks and benefits. *Nat. Rev. Endocrinol. 9*, 216−227.

(3) Potts, J. T., jr, Kronenberg, H. M., and Rosenblatt, M. (1982) Parathyroid hormone: chemistry, biosynthesis, and mode of action. *Adv. Protein Chem. 35*, 323−396.

(4) Potts, J. T., jr, Tregar, G. W., Keutmann, H. T., Niall, H. D., Sauer, R., Deftos, L. J., Dawson, B. F., Hogan, M. L., and Aurbach, G. D. (1971) Synthesis of a biologically active N-terminal tetratriacontapeptide of parathyroid hormone. *Proc. Natl. Acad. Sci. U. S. A. 68*, 63−67.

(5) Lane, J. M., Russell, L. K., and Khan, S. N. (2000) Osteoporosis. *Clin. Orthop. Relat. Res. 372*, 139−150.

(6) Kristensen, M., Foged, C., Berthelsen, J., and Nielsen, H. M. (2013) Peptide-enhanced oral delivery of therapeutic peptides and proteins. *J. Drug Delivery Sci. Technol. 23*, 365−373.

(7) Morishita, M., Kamei, N., Ehara, J., Isowa, K., and Takayama, K. (2007) A novel approach using functional peptides for efficient intestinal absorption of insulin. *J. Controlled Release 118*, 177−184.

(8) Kamei, N., Morishita, M., Eda, Y., Ida, N., Nishio, R., and Takayama, K. (2008) Usefulness of cell-penetrating peptides to improve intestinal insulin absorption. *J. Controlled Release 132*, 21−25.

(9) Khafagy, E.-S., and Morishita, M. (2012) Oral biodrug delivery using cell-penetrating peptide. *Adv. Drug Delivery Rev. 64*, 531−539.

(10) Liang, J. F., and Yang, V. C. (2005) Insulin-cell penetrating peptide hybrids with improved intestinal absorption efficiency. *Biochem. Biophys. Res. Commun. 335*, 734−738.

(11) Patel, L., Wang, J., Kim, K., and Borok, Z. (2009) Conjugation with cationic cell-penetrating peptide increases pulmonary absorption of insulin. *Mol. Pharmaceutics 6*, 492−503.

(12) Caldinelli, L., Albani, D., and Pollegioni, L. (2013) One single method to produce native and Tat-fused recombinant human α-synuclein in Escherichia coli. *BMC Biotechnol. 13*, 32.

(13) Zigoneanu, I. G., and Pielak, G. J. (2012) Interaction of α-synuclein and a cell penetrating fusion peptide with higher eukaryotic cell membranes assessed by ^{19}F NMR. *Mol. Pharmaceutics 9*, 1024−1029.

(14) Derossi, D., Calvet, S., Trembleau, A., Brunissen, G. C., and Prochiantz, A. (1996) Cell internalization of the third helix of the Antennapedia homeodomain is receptor-independent. *J. Biol. Chem. 271*, 18188−18193.

(15) Frankel, A., and Pabo, C. (1988) Cellular uptake of the tat protein from human immunodeficiency virus. *Dis. Markers 8*, 1189−1193.

(16) Elliott, G., and O'Hare, P. (1997) Intercellular trafficking and protein delivery by a herpesvirus structural protein. *Cell 88*, 223−233.

(17) Ryser, H. J., and Hancock, R. (1965) Histones and basic polyamino acids stimulate the uptake of albumin by tumor cells in culture. *Science 150*, 501−503.

(18) Marx, U. C. (1998) Structure-activity relation of NH2-terminal human parathyroid hormone fragments. *J. Biol. Chem. 273*, 4308−4316.

(19) Rydberg, H. A., Matson, M., Amand, H. L., Esbjörner, E. K., and Nordén, B. (2012) Effects of tryptophan content and backbone spacing on the uptake efficiency of cell-penetrating peptides. *Biochemistry 51*, 5531−5539.

(20) Bahnsen, J. S., Franzyk, H., Sandberg-Schaal, A., and Nielsen, H. M. (2013) Antimicrobial and cell-penetrating properties of penetratin analogs: Effect of sequence and secondary structure. *Biochim. Biophys. Acta 1828*, 223−232.

(21) Christiaens, B., Grooten, J., Reusens, M., Joliot, A., Goethals, M., Vandekerckhove, J., Prochiantz, A., and Rosseneu, M. (2004) Membrane interaction and cellular internalization of penetratin peptides. *Eur. J. Biochem. 271*, 1187−1197.

(22) Schellekens, H. (2002) Bioequivalence and the immunogenicity of biopharmaceuticals. *Nat. Rev. Drug Discovery 1*, 457−462.

(23) Kane, J. F., and Hartley, D. L. (1988) Formation of recombinant protein inclusion bodies in Escherichia coli. *Tibtech. 6*, 95−101.

(24) Georgiou, G., Telford, J. N., Shuler, M. L., and Wilson, D. B. (1986) Localization of inclusion bodies in Escherichia coli over-producing beta-lactamase or alkaline phosphatase. *Appl. Environ. Microbiol. 52*, 1157−1161.

(25) Singh, S. M., and Panda, A. K. (2005) Solubilization and refolding of bacterial inclusion body proteins. *J. Biosci. Bioeng. 99*, 303−310.

(26) Taylor, G., Hoare, M., Gray, D. R., and Marston, F. A. O. (1984) Size and density of inclusion bodies. *Nat. Biotechnol. 4*, 553−557.

(27) Pellegrini, M., Royo, M., Rosenblatt, M., Chorev, M., and Mierke, D. F. (1998) Addressing the tertiary structure of human parathyroid hormone-(1−34). *J. Biol. Chem. 273*, 10420−10427.

(28) Strickland, L. A., Bozzato, R. P., and Kronis, K. A. (1993) Structure of human parathyroid hormone(1−34) in the presence of solvents and micelles. *Biochemistry 32*, 6050−6057.

(29) Marx, U. C., Adermann, K., Bayer, P., Forssmann, W. G., and Rösch, P. (2000) Solution structures of human parathyroid hormone fragments hPTH(1−34) and hPTH(1−39) and bovine parathyroid hormone fragment bPTH(1−37). *Biochem. Biophys. Res. Commun. 267*, 213−220.

(30) Caulfield, M. P., McKee, R. L., Goldman, M. E., Duong, L. T., Fisher, J. E., Gay, T. C., DeHaven, P. A., Levy, J. J., Roubini, E., Nutt, R. F., Chorev, M., and Rosenblatt, M. (1990) The bovine renal parathyroid hormone (PTH) receptor has equal affinity for two different amino acid sequences: the receptor binding domains of PTH and region. *Endocrinology 127*, 83−87.

(31) McKee, M. D., and Murray, T. M. (1985) Binding of intact parathyroid hormone to chicken renal plasma membranes. *Endocrinology 117*, 1930−1939.

(32) Tünnemann, G., Ter-Avetisyan, G., Martin, G. M., Stoockl, M., Hermann, A., and Cardoso, C. (2008) Live-cell analysis of cell penetration ability and toxicity of oligo-arginines. *J. Pept. Sci. 14*, 469−476.

(33) Bendifallah, N., Rasmussen, F. W., Zachar, V., Ebbesen, P., Nielsen, P. E., and Koppel (2006) Evaluation of cell-penetrating peptides (CPPs) as vehicles for intracellular delivery of antisense peptide nucleic acid (PNA). *Bioconjugate Chem. 17*, 750−758.

(34) Pujals, S., Fernández-Carneado, J., López-Iglesias, C., Kogan, M. J., and Giralt, E. (2006) Mechanistic aspects of CPP-mediated intracellular drug delivery: Relevance of CPP self-assembly. *Biochim. Biophys. Acta 1758*, 264−279.

(35) Savitsky, P., Bray, J., Cooper, C. D. O., Marsden, B. D., Mahajan, P., Burgess-Brown, N. A., and Gileadi, O. (2010) High-throughput production of human proteins for crystallization: the SGC experience. *J. Struct. Biol. 172*, 3−13.

(36) Lutz, M. B., Kukutsch, N., Ogilvie, A. L. J., Rössner, R., Koch, F., Romani, N., and Schuler, G. (1999) An advanced culture method for generating large quantities of highly pure dendritic cells from mouse bone marrow. *J. Immunol. Methods 223*, 77−92.

DOI: 10.1021/bc5005763
Bioconjugate Chem. 2015, 26, 477−488

(37) Foged, C., Franzyk, H., Bahrami, S., Frokjaer, S., Jaroszewski, J. W., Nielsen, H. M., and Olsen, C. A. (2008) Cellular uptake and membrane-destabilising properties of alpha-peptide/beta-peptoid chimeras: lessons for the design of new cell-penetrating peptides. *Biochim. Biophys. Acta 1778*, 2487–2495.
(38) Cory, A. H., Owen, T. C., Barltrop, J. A., and Cory, J. G. (1991) Use of an aqueous soluble tetrazolium/formazan assay for cell growth assays in culture. *Cancer Commun. 3*, 207–212.

DOI: 10.1021/bc5005763
Bioconjugate Chem. 2015, 26, 477–488